The Role of Noise in Some Physical and Biological Systems

J. D. Gunton[1], R. Toral[2,3], Claudio Mirasso[3], and M. E. Gracheva[4]

[1]Department of Physics, Lehigh University, Bethlehem, PA 18015, USA
[2] Instituto Mediterraneo de Estudios Avanzados, CSIC-UIB,
Ed. Mateu Orfila, Campus UIB, E-07122 Palma de Mallorca, Spain
[3]Departament de Física, Universitat de les Illes Balears,
E-07122 Palma de Mallorca, Spain
[4]School of Mathematics, University of Minnesota,
Minneapolis, MN 55455, USA

March 7, 2003

Abstract

A short review of our recent research involving the role of noise in a variety of systems is given. Two classes of problems are discussed. The first is the effect of fluctuations on cellular and intercellular calcium oscillations. Oscillations in intracellular and intercellular calcium ion concentrations are responsible for the regulation of a remarkable number of different cellular processes in the human body. Fluctuation effects that are ignored in deterministic models of these oscillations are discussed. The second class includes two examples of coherence resonance, in which noise induces some type of order in systems in the absence of periodic forcing. The two examples reviewed include system size resonance and coherence resonance in chaotic systems. System size resonance (coherence resonance that depends on the number of elements of the system) is demonstrated for a globally coupled FitzHugh-Nagumo model. Coherence resonance in chaotic systems is illustrated for the Chua circuit.

1 Introduction

It has long been recognized that noise plays an important role in many areas of science. Its origins go back to the work of Einstein and Langevin on the theory of the random (Brownian) motion of a small particle immersed in a fluid. In particular, Langevin developed a theory of the particle motion in which he separated the total force on the particle into a systematic part (a damping frictional force) and a fluctuating part (or noise). Since these forces result from the surrounding environment of the particle, they are in fact related by a fluctuation-dissipation theorem. Langevin assumed that the noise satisfied a Gaussian distribution and from this obtained a detailed description of the particle motion, including various time correlation functions. The concept of a random force, specified by some assumed probability distribution function, has proved to be of great theoretical value. During the past decades there have been enormous developments in both the application and theory of stochastic processes [1, 2, 3].

The effects of noise are in general of two different kinds. On one hand, noise can be somewhat deleterious and produce small changes to deterministic behavior that might alter an otherwise synchronized behavior. Modern communication, for example, is hindered by background noise. On the other hand, there is now an abundance of examples in which noise actually can enhance order in the dynamical behavior of a system. Both effects are important to understand and this short review will deal with examples of both, involving our own recent research activities.

That noise can have a *constructive* role has been one of the more important discoveries of the last decades in the field of stochastic processes. The pioneering example of this is that of *stochastic resonance* [4, 5], in which a bistable system shows an optimal response (resonance) to a weak, periodic forcing due to the influence of noise. In addition to stochastic resonance, purely temporal dynamical systems can exhibit a variety of behavior, such as noise-induced transitions [6] or noise-induced transport [7]. In spatially extended systems, noise is now known to induce a large variety of ordering effects [2], such as pattern formation [8, 9], phase transitions [10, 11, 12], phase separation [13, 14], spatiotemporal stochastic resonance [15, 16] and noise-sustained structures [17, 18]. In all these cases, some type of *order* appears **only** in the presence of the right amount of noise.

The more common, degrading, effect of noise, is ubiquitous and remains important to understand. It has many manifestations in nature, including in many aspects of biology, such as cell biology, where fluctuations can play a non-trivial role. In this short review article we discuss examples of each that have relevance in physical and biological systems and that have been the subject of our own recent research: oscillation in calcium ions and noise induced resonances.

1.1 Oscillations in intracellular and intercellular calcium ions

Oscillations in the intracellular and intercellular calcium ion concentrations are responsible for the regulation of a remarkable number of different cellular processes in the human body. Ca^{2+} is crucial to the fertilization, development and differentiation of cells, muscle contraction, metabolic processes and gene expression. It is in fact a remarkable intracellular and intercellular messenger, whose versatility is still only partially understood. A recent review of its importance and universality [19] is given in an article entitled "*Calcium-a life and death signal*", whose authors note that almost everything we do is controlled by Ca^{2+}. Cellular Ca^{2+} concentrations are typically about 100 nM at rest, but rise to concentrations of roughly ten times this when stimulated. Such increases can be produced by ligands (agonists) binding to receptors located on the plasma membrane, through a process involving the second messenger inositol-1,4,5-trisphosphate (IP_3). An important characteristic of the spike-like Ca^{2+} oscillations is that they are primarily frequency, rather than amplitude, encoded. Thus an increase in the agonist concentration increases the frequency of oscillation, but has little effect on its amplitude. Calcium signals can also be propagated between cells, providing an important means of cell communication. Such intercellular communication can take different forms, including diffusion of calcium or IP_3 through gap junctions and paracrine (indirect) signaling.

Considerable success has been realized in understanding these intracellular oscillations through the use of deterministic equations for various intracellular biochemical processes. These can be extended to describe the synchronization of oscillations between cells via gap junction diffusion or indirect

signaling. A recent comprehensive review of the modelling of cellular oscillations is given in [20]. Deterministic models, however, ignore the fluctuations in the concentration of molecular species and the fact that chemical reactions are stochastic processes, that occur with certain rates. Since the number densities of the intracellular signaling molecules are typically low (of the order of $1 - 10^2 \mu m^{-3}$, stochastic effects can be important. Such fluctuations, for example, are responsible for the observed variation in the amplitudes and widths of the Ca spikes; they also affect the synchronization of cells via calcium signaling. In what follows we describe recent work on the role of noise in two different types of intercellular calcium signaling [21, 22]. Other recent studies of stochastic effects in cellular calcium oscillations are given in [23, 24, 25].

1.2 Stochastic and coherence resonance

When a dynamical system is subjected to an external periodic forcing, it is well known that synchronization between the system and the forcing can occur under a wide range of circumstances. A resonance is defined as a maximum in the response of the system when varying some control parameter (for instance, the frequency of the external signal). One might naively believe that fluctuations, either in the input or in the intrinsic dynamics, would worsen the quality of the synchronization. However, it is now well established that, in certain situations, the response of a nonlinear dynamical system to an external forcing can actually be *enhanced* by the presence of noise (fluctuations).

We first describe briefly the phenomenon of stochastic resonance and the related phenomenon of coherence resonance, as these provide examples of the powerful constructive role of noise. The paradigm of stochastic resonance involves the motion of a heavily damped particle, moving in a symmetric double well potential V(x). If one couples this particle to a heat bath at temperature T, then the particle becomes subject to stochastic forces that cause jumps between the two wells. with a rate first predicted by Kramers [26]. The jump rate is proportional to $\exp\left(-\frac{\Delta V}{k_B T}\right)$, where ΔV is the height of the barrier separating the two minima and the noise strength $D = k_B T$ (where k_B is the Boltzmann constant). Now imagine applying a weak, periodic force of frequency ω to the particle. This tilts the double well potential

asymmetrically up and down, periodically raising and lowering the potenstial barrier. Since the periodic force is weak, it does not cause the particle to roll periodically from one minima to another. On the other hand, the noise-induced jumps between the two wells can become synchronized with the periodic forcing. Namely, if one varies the frequency of the forcing term such that the average waiting time between two noise induced jumps is equal to half the period of the forcing term, one can achieve synchronized resonance. In this case there is a coordination of the noise-acted jumps between the potential minima with the weak periodic forcing. There is by now an abundance of examples of stochastic resonance in many fields of science and engineering. A recent, thorough review of this topic is given by Gammaitoni et al [3].

The related phenomena of coherence resonance, with which we will be concerned, is a noise induced resonance that occurs in the absence of periodic forcing. A typical example involves the role of noise on an excitable system. Important biological examples of excitable systems include the Hodgkin-Huxley model and the closely related FitzHugh-Nagumo model [27] of cellular electrical activity. Although these models were originally developed to describe nerve pulses, they have been subsequently used for modelling of spiral waves in two dimensional excitable medium. An excitable system is one in which its rest state (corresponding to a fixed point which is a basin of stable attraction) is linearly stable against a perturbation. If the perturbation is sufficiently large, however, the system undergoes a large excursion of its variables (for the FitzHugh-Nagumo model this represents a nerve pulse) in phase space before returning to its rest state. The total time between pulses, t_p, is the sum of two times: the excursion time t_e (the time needed to return from the excited state to the fixed point) and the activation time (the time needed to excite the system from its fixed point), t_a. These two times and their fluctuations have a different dependence on the noise amplitude [28]. By analyzing the behavior of each of these for small and large noise, respectively, one can conclude that the normalized variance ("jitter") in the fluctuations should have a minimum as a function of the noise amplitude. This coherence resonance is a nonlinear response of the system to purely noise excitation. A similar effect, although induced by a different physical mechanism, is that of stochastic resonance without external periodic force which can occur in a system near a limit cycle bifurcation point [29, 30].

We will focus in this article on two particular cases in which noise plays a constructive role: coherence resonance in chaotic systems and so-called system size resonance, in which coherence resonance depends on the number of elements of the system.

2 Stochastic effects in cellular calcium oscillations

A number of theoretical models have been developed to explain intracellular Ca oscillations [31, 32, 33, 34, 35]. The basis for most of these is that after an agonist (hormone) binds to the extracellular side of a receptor bound to the membrane, the G_α subunit at the intracellular side of the receptor-coupled G-protein is activated. This activated G-protein then stimulates a phospholipase C which helps forming a second messenger IP_3 and diacylglycerol. IP_3 then binds to specific receptors in the membrane of an internal store of calcium (such as the endoplasmic reticulum). The binding helps the opening calcium channels, which leads to a large flux of calcium ions from the internal store into the cytosol, which then stimulates the release of additional calcium ions. Some details of this complex progress, however, remain unknown. One of the earliest and simplest models is the so-called minimal model, which is an example of a calcium-induced, calcium release model [31, 32, 33]. As we use this in our discussion below, we briefly describe this model here.

In this model, the calcium cell dynamics is described by two differential equations for the cytosolic Ca^{2+} concentration, y_1, and the internal store of Ca^{2+}, y_2:

$$\frac{dy_1}{dt} = V_0 + \beta_1 V_1 - V_2 + V_3 + k_f y_2 - k y_1 \quad (1)$$

$$\frac{dy_2}{dt} = V_2 - V_3 - k_f y_2 \quad (2)$$

where V_2 and V_3 are certain nonlinear functions of y_1 and y_2 that depend on several parameters. These rates describe, respectively, the pumping of Ca^{2+} into an IP_3-insensitive store and the release of Ca^{2+} from that store into the cytosol. The latter is a process activated by the cytosolic Ca^{2+}. The term V_0 describes a constant input of Ca^{2+} from the extracellular medium into the cytosol, while the term $\beta_1 V_1$ describes the IP_3 modulated release of Ca^{2+}

from an IP_3 sensitive store. The parameter k_f is a rate constant describing a linear leak of y_2 into y_1, while k describes the linear transport of Ca^{2+} into the extracellular medium.

This model has been studied extensively [31, 32]. It is known that for a given set of the parameter values Ca^{2+} oscillations will occur when the parameter β_1, which increases with the concentration of the external hormonal stimulus, lies in a range $\beta_{min} < \beta_1 < \beta_{max}$. That is, there is a Hopf bifurcation from a steady state solution to a periodic solution at β_{min}, followed by a second Hopf bifurcation back to a steady state solution at β_{max} (these minimum and maximum values depend mainly on the parameters V_0 and V_1). The frequency of the oscillation depends on the value of β in the region between these minimum and maximum values. This model provides a useful starting point for a description of Ca^{2+} oscillations, although it has subsequently been replaced by more detailed models of the intracellular biochemical processes.

2.1 Intercellular calcium spiking in hepatocytes

Recent experimental studies revealed the coordination of calcium oscillations in heterogeneous hepatocyte cells [36, 37]. The authors of there references studied the mechanisms that control the coordination and intercellular propagation of calcium waves induced in rat hepatocytes (studying propagation of such intercellular Ca^{2+} waves in doublet and triplet cells). Initially they investigated [36] calcium waves induced by noradrenaline and showed that gap junction coupling is necessary for the coordination of the oscillations between the different cells. They also demonstrated that it is necessary to have hormone stimulation at each hepatocyte in order to have cell-cell calcium signal propagation. Furthermore, they found that there were functional differences between adjacent hepatocytes. In a subsequent paper [37] they continued these studies, combining single-cell studies with experiments on cell populations isolated from the peripheral (periportal) and central (perivenous) zones of the liver cell plate. They found strong evidence that the sequential pattern of calcium responses to vasopressin in these multicellular rat hepatocyte systems was due to a gradient of cell sensitivity (from cell to cell) for the hormone. The first cell to respond had the greatest sensitivity to the global stimulus, while the last cell to respond had the least sensitivity. This is an important observation, since such gradients may impose an orientation

on calcium waves in liver cells and provide a pacemaker-like mechanism for regulating intercellular communication in the liver. Based upon these experimental studies, two theoretical models have been proposed. The first is due to Dupont et al [38], whose deterministic model of coupled differential equations is based on junctional coupling of multiple hepatocytes which differ in their sensitivity to the hormonal stimulus. As a consequence of this difference, the intrinsic frequency of intracellular calcium oscillations also varies from cell to cell. These oscillators are coupled by an intercellular messenger, which could be either Ca^{2+} or inositol 1,4,5-trisphosphate IP_3. The model yielded intercellular waves that were confirmed experimentally [38]. The authors also provided experimental evidence that the degree of synchronization is greater for the first few spikes, in agreement with the prediction of their model.

Höfer [39] proposed an alternative deterministic model to explain the experimental results, based on the assumption that the rather large variation in the intrinsic oscillator frequencies found in the experimental studies resulted from random heterogeneities in the structural properties of the cells (such as their sizes, shapes and endoplasmic reticulum content). He assumed that the concentration of the second messenger IP_3 rapidly reaches a steady-state value (different for different cells) that is considered as one of the parameters of the model. He also assumed that the intercellular synchronization was due to a flux of Ca^{2+} between cellular gap junctions. After certain approximations he obtained a deterministic model for the time evolution of the average cytosolic calcium concentration, x_j, and the average calcium concentration of the j-th cell, z_j. For the case in which only two cells are coupled, the rather complicated equations take the form

$$\frac{dx_j}{dt} = f(x_j, z_j) + \gamma(x_i - x_j) \tag{3}$$

$$\frac{dz_j}{dt} = g(x_j, z_j) + \gamma(x_i - x_j) \tag{4}$$

where the functions f and g are specific nonlinear functions of x_j and z_j The last term, proportional to γ, describes the diffusion between cells. γ is a junctional coupling coefficient and is proportional to the gap-junctional permeability. The indices can adopt the values $(i, j) = (1, 2)$ and $(2, 1)$. The model can be easily generated to the case of more than two cells. An important parameter in these equations is the IP_3 concentration in cell j. The equa-

tions also contain In the functions f and g) the parameters $\rho_j = A^j_{PM}/C^j_C$, $\alpha_j = A^j_{ER}/A^j_{PM}$ and $\beta_j = C^j_{ER}/C^j_C$ which define various structural characteristics of the j-th cell and account for the heterogeneous behavior of different cells. The variables A^j_{ER} and A^j_{PM} are the areas of the endoplasmatic reticulem and plasma membrane of cell j respectively. The details of the model are given in [39]. Höfer showed that this model yields results for two and three coupled cells that are in good agreement with many of the experimental results of Tordjmann et al [36, 37]. However, as in the case of the Dupont et al study [38], there are observed differences that one could ascribe to the role of noise. This led to our own work [21].

To understand the limitations of deterministic models such as the above, note that these completely ignore the fluctuations that result from the fact that chemical reactions do not occur uniformly nor continuously in time. To consider the effects of such fluctuations, we studied stochastic versions of both models. Rather than adding noise to these models, we found a better approach in a Monte Carlo method developed by Gillespie [40, 41]. Gillespie took into account the facts that the concentration of a molecular species can only vary by a discrete amount (rather than continuously, as assumed above) and that a chemical reaction is itself a stochastic process, that occurs with a certain rate. Therefore one cannot determine which of several reactions will occur next. One can only determine the probability that a given reaction will take place. Thus one introduces rate constants corresponding to the various terms in the differential equations and also defines

$$x_j = \frac{X_j}{\Omega}; \quad z_j = \frac{Z_j}{\Omega} \tag{5}$$

Ω is the volume of the cytosolic compartment of the cell; fluctuation effects will obviously be more important for small Ω. In the limit of Ω tending to infinity, the stochastic model yields the same results as the deterministic model, as the effects of such fluctuations become negligible. The population numbers X_j and Z_j can vary by discrete, integer, amounts according to some probability that reflects the possible reactions taking place in the system. The possible events and their reaction constants are defined in [21]. We then carried out a Monte Carlo simulation of the stochastic version of the deterministic models of Höfer and Dupont et al. We will illustrate some of our results for Höfer's taking the value $\Omega = 300\,\mu m^3$ for the cytosolic cell volume. Fig. 1 compares the calcium oscillations for one isolated cell in our

stochastic model for $\Omega = 300\,\mu m^3$ and $10^5\,\mu m^3$ respectively. Note from this figure that the stochastic effects are important for $\Omega = 300\,\mu m^3$ whereas the result for large $\Omega = 10^5\,\mu m^3$ agrees with the deterministic limit.

Next we studied the behavior of two connected hepatocytes which are globally stimulated. The calcium oscillations in the two cells are totally uncoordinated if the membrane permeability is set to zero, as should be the case (Fig. 2a). For a value of the permeability γ=0.07 s^{-1} we found 1:1 locking (Fig. 2b). We also found agreement with Höfer's results in the limit of large Ω, as is to be expected.

We also simulated an aspect of the experiment in which the membrane permeability between cells was blocked for a time interval (after oscillations were established) in such a way as to prevent Ca^{2+} from passing through the membrane (γ is set to zero in the model). In this case the cells lost their synchronization, but after washing the chemical responsible for the blocking, the cells regained synchronization. Our simulations confirmed this behavior and also showed a variation in the amplitude of oscillations and fluctuations in the baseline value of Ca^{2+}, in agreement with the experimental results [37]. These effects are absent in the deterministic limit of the model.

Finally, we modelled the experimental study of a triplet of hepatocytes, in which one can also see synchronized intercellular signaling. However, if a heparin treatment is applied to the intermediate cell the calcium oscillations of the middle cell are altered. In addition, the synchronized spiking between the first and third cells is destroyed. Fig. 3 (fig3i.ps) shows the results of our simulation. It can be seen that after the heparin application at $t = 200\ s$, calcium oscillations were no longer present in the second cell. In addition, the first and third cells in the triplet spike asynchronously. These results are in good agreement with the experimental results [37].

2.2 A model of unidirectional, paracrine calcium signalling

In general, the signalling between cells is bidirectional, as in the model discussed above. However, there is a recent experiment [42, 43] in which the authors deliberately produce a unidirectional signalling, by setting up so-

called "donor" and "sensor" cells. The oscillations induced in the donor cells by an agonist input were shown to produce oscillations in the sensor cells via an indirect (paracrine) signalling mechanism. In an attempt to explain these experimental results, we proposed a simple deterministic model which we studied by numerical means [22]. We also studied the effects of fluctuations, using the method of Gillespie described above. Our results were in qualitative agreement with the experimental results, in terms of predicting the observed unidirectional signalling. In addition, however, we found a "Devil's Staircase" behavior for both the deterministic and stochastic versions of the model (in the latter case, for reasonable choices of the cell volume). The Devil's Staircase behavior has not yet been observed experimentally.

We first briefly describe the experiment [42]. The system studied is in itself a "model" system, in that it is composed of two different cell types with quite different properties. The first are "sensor" (HEK293) cells which have been stably transfected with extracellular-sensing receptors (CaRs). These CaRs are coupled to the phospho-inositide pathway, but are insensitive to hormonal stimulation. The second are "donor" (BHK-21) cells, which have have **not** been transfected with CaRs. In contrast to the first cell type, these cells are sensitive to hormonal stimulation by AVP, 5HT or histamine. This specially prepared cellular system thus allows the distinction between "donor" cells (BHK-21 cells, not transfected, but able to respond to a hormonal stimulus) and "sensor" cells (HEK293 cells, transfected, but unable to respond to the hormonal stimulus). These two cell types were maintained in close proximity. Histamine was then added to the bath, producing calcium oscillations in the BHK cells. Less than 10 seconds later, calcium oscillations were observed in nearby HEK-CaR cells. As there was no gap-junction communication, the authors interpreted their results as providing evidence for a gap-junction-independent mode of intercellular communication, mediated by CaR and extracellular Ca^{2+}.

As one still does not understand in detail the complex biochemistry involved in the CaR coupling, we considered a simplified model that might capture the qualitative features of this new form of signalling. There are two aspects to describing the intercellular communication: the intracellular dynamics and the coupling between cells. As there are many different models for the intracellular calcium oscillations, we chose the simplest, i.e. the minimal model discussed above. We coupled two such cells, the donor cell and the sensor

cell, by assuming that the stimulus of the target cell is proportional to the cytosolic calcium content of the first cell. Since some of the cytosolic Ca^{2+} produced in the donor cell is extruded into a small space near a CaR receptor, this seems to be a reasonable assumption. This avoids modeling the extracellular diffusion of Ca^{2+} as well as the complex receptor dynamics that is presumably involved in the calcium-sensing receptor mechanism proposed by Höfer et al. [42]. However, our model is consistent with the spirit of the single cell minimal model in that it provides a minimal two cell coupling that yields interesting intercellular communication. We should also note that under *in vivo* conditions, hormones are not released steadily, but are released in a pulsatile fashion. Thus our results for the sensor cell responding to an input signal are also applicable to the physiologically interesting question of how the intracellular cytosolic calcium responds to a pulsatile application of agonists.

The donor cell dynamics is described by two differential equations for its cytosolic Ca^{2+} concentration, y_1 and its internal store of Ca^{2+}, y_2, given in equations (1) and (2). The sensor cell is modelled using the same equations for its cytosolic and internal calcium concentrations $y_1^{'}$ and $y_2^{'}$ as given in Eqs. (1) and (2). However, instead of a term $\beta_2 V_1'$ representing a constant stimulus, we use the term $\beta_2 y_1 V_1'$, which provides the coupling between the cells. This assumes that the stimulus to the sensor cell from the extruded calcium from the donor cell is proportional to the latter's cytosolic calcium concentration. In general, the structural parameters V_0, V_1, V_2, V_3, k_f, k of the first cell and V_0', V_1', V_2', V_3', k_f', k' of the second cell can be different, but for the sake of simplicity we took them to be the same. We found in general that oscillations in the donor cell due to a constant hormonal input produce oscillations in the sensor cell. This is in qualitative agreement with the experimental observation [42], but the detailed predictions of our model require further experimental study.

We calculated the N:M rhythms predicted for this coupled minimal model as a function of β_1 for fixed β_2, where N denotes the number of stimuli arising from the donor cell and M the number of responses of the sensor cell in a given time interval. For example, the frequency of response can be the same as the frequency of the stimulus, i.e. N:M is 1:1. However, in general the Ca^{2+} response in the sensor cell is blocked when the frequency of pulses of the donor cell is increased. Fig. 4 shows a 3:2 response. This phenomenon of

blocking is also seen in heart patients, where it is known as Wencekbach periodicity. As one varies β_1 the sensor cell passes through a sequence of N:M phase locked regimes (in response to the oscillatory stimuli from the donor cell) and exhibits a "Devil's staircase" behavior [30], as shown in Fig. 5. That is, between any two steps there is a countless number of staircases [44] This response of the sensor cell is similar to experimental results of Schöfl et al. [45] who applied square wave pulses of phenylephrine to liver cells every 30 seconds. They found stimulus/response rhythms such as 2:1, but with less regularity than shown here [23]. A subsequent stochastic study based on a deterministic model of intracellular dynamics due to Chay et al [34] yielded results qualitatively similar to the experiment [23].

We also studied a stochastic version of our model, using Gillespie's method [40], for different values of the cell volume Ω (assumed to be the same for both cells). For very small Ω fluctuations destroy the phase locking, while in the limit of large Ω one recovers the deterministic limit. Both results are what one would expect. For intermediate values of Ω, however, such as $\Omega = 2000\mu m^3$, which is the approximate volume of hepatocyte cells, we find that phase locking persists, although with occasional lapses. Some typical results for this case are shown in Fig. 6. Thus we find a stochastic version of the Devil's staircase for values of the cell volume that are realistic. We also found that cells can switch between frequencies in the stochastic model if we choose β_1 and β_2 such that the deterministic model would give a frequency locking of the cells on the edge of one of the steps of the Devil's staircase. Hopefully this work will lead to further experimental investigations of the possibility of a Devil's Staircase behavior in cellular calcium oscillations.

3 System size resonance

System size resonance is a type of coherence resonance in which the resonance occurs for a specific number of elements of the system [52, 53, 54, 25]. In this section, we review our work on system size resonance in the FitzHugh-Nagumo model [47]. As noted earlier, this model provides a simple representation of firing dynamics and has been widely used as a prototypic model for spiking neurons. It has also been used to describe certain aspects of cardiac cells [48, 49]. Our model is a set of N FitzHugh–Nagumo systems that we

couple through a long-range, global interaction:

$$\epsilon \dot{x_i} = x_i - \frac{1}{3}x_i^3 - y_i + \frac{K}{N}\sum_{j=1}^{N}(x_j - x_i) \quad (6)$$

$$\dot{y_i} = x_i + a + D\xi_i(t) \quad (7)$$

where independent noises of intensity D have been added to the variables y_i as in ref. [28]. The small parameter ϵ introduces a difference in the time scales of x_i and y_i, with x_i and y_i being the fast and slow variables, respectively. As usual, we choose the $\xi_i(t)$ to be white noises with Gaussian distribution of zero mean and correlations $\langle \xi_i(t)\xi_j(t')\rangle = \delta_{ij}\delta(t-t')$. The systems are globally coupled by a gap-junctional form, as indicated by the last term of Eq.(6), where K is the coupling strength. Similar globally coupled models have been used previously to study array enhanced stochastic resonance in the coupled FitzHugh-Nagumo equation [50].

The case of interest is the excitable regime, $a > 1$. In that case, as discussed in the introduction, if $K = 0$ each system emits (nerve) pulses that are trajectories in phase space triggered by the noise term. Coherence resonance occurs when the regularity of the time between pulses is optimal for a certain value of the noise intensity D [28]. The behavior is the same for all the systems for $K = 0$; there is, of course, no correlation between the responses of individual systems.

To study the collective response of the **coupled** system, we introduce the average values of the activator and inhibitor variables as

$$X(t) = \frac{1}{N}\sum_{i=1}^{N} x_i(t) \quad (8)$$

$$Y(t) = \frac{1}{N}\sum_{i=1}^{N} y_i(t) \quad (9)$$

One can get a qualitative understanding of the origin of system size resonance for this model by following an approach by Desai and Zwanzig [51] (see also reference [52]). This approach leads to an approximate equation for these average values of the form:

$$\epsilon \dot{X} = F(X, K) - Y \quad (10)$$

$$\dot{Y} = X + a + \frac{D}{\sqrt{N}}\xi(t) \quad (11)$$

where $\xi(t)$ is a white noise source. The exact form of the function $F(X,K)$, which depends on the global variable X as well on the coupling strength K, is not necessary for the qualitative argument. We need only observe that in the (exact) equation for $Y(t)$ the noise intensity appears rescaled as $D/\sqrt{N}$. Therefore, this approximation suggests that the optimal effective noise intensity for the appearance of coherence resonance can be achieved by varying the number of coupled elements N, as in the case of stochastic resonance for the bistable system considered in [52].

To obtain a quantitative description of this system size resonance, we numerically integrated the equations of motion (6) and (7). Our results are summarized as follows: The left panel of Fig. 7 shows the temporal behavior for the variable $X(t)$ while the right panel of the same figure shows the temporal behavior for the variable $x_i(t)$ of one of the elements chosen randomly, for three different values of the number of coupled elements (see the caption of the figure for details of the parameters). Notice that for $N = 160$ the regularity of the emitted pulses peaks is better than that corresponding to larger or smaller values of N. This is a clear signature of coherence resonance. It can also be seen that the regularity in the averaged variable $X(t)$ is better than in one of the individual elements, showing that the coupling allows for a smoothness of the temporal behavior. It is worth noting that the peaks in the collective variable $X(t)$ and $x_i(t)$ are very well synchronized in time indicating that the individual systems are pulsing synchronously in time. In Fig. 8 (left panel) we show the temporal behavior for the slow variable $Y(t)$, as well as a time trace for a single $y_i(t)$ (right panel). In contrast with the fast variable X, the averaged slow variable $Y(t)$ shows a nice regular behavior for an intermediate number of elements, while the individual traces $y_i(t)$ do not.

We computed various quantities commonly used to quantify the coherence resonance effect[28]. We show only one here, namely the time correlation function $C_X(t)$ of the averaged X variable, defined as

$$C_X(t) = \frac{\langle \delta X(t') \delta X(t+t') \rangle}{\langle \delta X(t')^2 \rangle} \tag{12}$$

$$\delta X(t) = X(t) - \langle X(t') \rangle \tag{13}$$

and similarly the correlation function $C_Y(t)$ for the averaged Y variable. Here the averages $\langle\,\rangle$ are with respect to the time t', after a small transient has

been neglected. Fig. 9 shows this correlation function for both the X and Y variables. It can be seen that the correlations extend further in time for an intermediate value, neither very large nor very small, of the number of coupled systems N. One can obtain a quantitative indicator of this effect from the characteristic correlation times τ_X and τ_Y for each variable as

$$\tau_{X,Y} = \int_0^\infty |C_{X,Y}(t)|\, dt \tag{14}$$

We found that both times reach a maximum at approximately the same value $N \approx 160$, indicating that, for the set of parameters chosen, the maximum extent of the time correlation occurs for this specific number of coupled excitable systems.

We also analyzed the *jitter* of the time between pulses [28]. A pulse in the $X(t)$ variable is defined when $X(t)$ exceeds a certain threshold value X_0 (taken arbitrarily as $X_0 = 0.3$, although other values yield similar results). The jitter R_X is defined as the root mean square of the time T_X between two consecutive pulses normalized to its mean value:

$$R_X = \frac{\sigma[T_X]}{\langle T_X \rangle} \tag{15}$$

and an equivalent definition for the jitter R_Y of the Y variable. The smaller the value of $R_{X,Y}$, the larger the regularity of the pulses (a value of $R_{X,Y} = 0$ indicates a perfectly periodic signal). We found that the jitter in each variable has a well defined minimum at a value of $N \approx 80$, again showing the existence of the system size resonance. We should also note that when comparing with the results of the correlation time, it is not uncommon that the two indicators (the correlation time τ and the jitter R) have their optimal values at different values of the system parameters [28, 55].

Since the FitzHugh–Nagumo system has been used previously to model some biologically relevant systems, we believe that our results, along the same lines as those of references [53, 54], can be relevant when analyzing the collective response of such systems in a noisy environment, and can help to explain the observed size of some groups of excitable cells in living organisms.

4 Coherence resonance in chaotic systems

Finally we discuss an interesting case in which one can have the main features of coherence resonance in *non excitable* systems. Namely, we recently showed [55, 56] that a Chua system, in a chaotic regime and in the presence of noise, can exhibit oscillations whose regularity is optimal for some intermediate value of the noise intensity. The Chua system with additive noise [57]can be written as:

$$\begin{aligned} \dot{x} &= \alpha(y - h(x)) \\ \dot{y} &= x - y + z \\ \dot{z} &= -\beta y - \gamma z + \xi(t) \end{aligned} \tag{16}$$

where $\xi(t)$ is as usual a Gaussian white noise, of zero mean and correlations $\langle \xi(t)\xi(t') \rangle = D^2\delta(t - t')$. The nonlinear function $h(x)$ is given by $h(x) = bx + \frac{a-b}{2}(|x + 1| - |x - 1|)$. We chose the values $a = -1/7$, $b = 2/7$, $\alpha = 4.60$, $\beta = 6.02$, $\gamma = 0$. For these values, the Chua system has two chaotic attractors: a single scroll and its mirror image. Depending on the initial conditions, the system will choose one attractor or the other. Thus, in the absence of fluctuations the attractors are independent and one cannot be reached from the other. The trajectories around each attractor have a well defined angular frequency ω_0, which for these values of the parameters is $\omega_0 \approx 3$.

If one numerically solves the above equations, one finds that noise produces a rather different behavior; the system now jumps back and forth between the two attractors. In Fig. 10 we show three trajectories of the variable $x(t)$ corresponding to increasing levels of the noise intensity. We observe three qualitatively different behaviors when increasing the noise level. For very small D (Fig. 10a) the average time of jumps between the attractors is large and the system spends most of the time rotating around one of these attractors. At the same time, the dispersion of the jumping time is also large. As D increases, approaching an optimum value (Fig. 10b), the system jumps between the two attractors more regularly. These jumps occur when the trajectory passes as close as possible to the other attractor. Finally, when D is very large, the system jumps more often but these jumps may start from different points of the trajectory and the behavior of the system is more irregular (Fig. 10c). The regularity already mentioned can be clearly observed

in Fig. 11 where we plot the variance of the residence time in each attractor, normalized to its mean value, as a function of the noise intensity. This curve exhibits a minimum at a noise level $D \approx 0.09$. It is also worth noting that following a jump from one attractor to the other, the new motion usually starts close to the center of that attractor, in an inner orbit. It is therefore not ready to jump to the other attractor until it reaches its outer orbit. This fact can be deduced from Fig. 10 by observing the time the system jumps from one attractor to the other.

We also calculated a variety of quantities that have been used to show the existence of coherence behavior. For example, we determined the correlation function, defined as $C(t) = [\langle x(t')x(t+t')\rangle - \langle x(t)\rangle^2]/[\langle x(t')^2\rangle - \langle x(t')\rangle^2]$, averaged over t', for the same noise intensities of Fig. 10. We found that for the optimum noise level the correlation function has the longest tail. We also calculated two other quantities: The correlation time τ_c, defined as $\tau_c = \int_0^\infty C(t)^2\, dt$ and the minimum of $C(t) \equiv C_m(t)$. For the entire range of noise levels considered, the former exhibits a local maximum at the optimum noise level, although almost hidden by the fact that τ_c is very large for very low noise level when the system remains most of the time rotating around one of the attractors. By contrast, $C_m(t)$ exhibits a clear minimum for the optimum noise level.

Although we have not discussed it here, one can also show that a simple model, composed of two separate limit cycles, is able to exhibit coherence resonance. Within this model one can in fact predict, e.g., the limits of $R(D)$ by a simple analytical approximation. The behavior of the chaotic Chua model follows qualitatively the results derived in the simple model,with coherence resonance illustrated by the dependence of several different quantities on the noise intensity.

These results show that the phenomenon of coherence resonance can be observed in a chaotic system. This is not an obvious conclusion since until recently the excitability has been considered to be a necessary ingredient for the existence of coherence resonance.

Acknowledgments: This work is supported by the Ministerio de Ciencia y Tecnología (Spain) and FEDER, projects BFM2001-0341-C02-01 and BFM2000-1108, and NSF grant DMR9813409.

References

[1] M. San Miguel, R. Toral, in *Instabilities and Nonequilibrium Structures VI*, eds. E. Tirapegui, J. Martínez and R. Tiemann, Kluwer Academic Publishers (2000).

[2] J. García–Ojalvo and J.M. Sancho, *Noise in Spatially Extended Systems* (Springer, New York, 1999).

[3] L. Gammaitoni, P. Hänggi, P. Jung and F. Marchesoni, Rev. Mod. Phys. **70**, 223 (1998).

[4] R. Benzi, A. Sutera and A. Vulpiani, J. Phys. **A14**, 453 (1981).

[5] C. Nicolis and G. Nicolis, Tellus **33**, 225 (1981).

[6] W. Horsthemke, R. Lefever, *Noise-Induced Transitions* (Springer, Berlin, 1984).

[7] P. Hänggi and R. Bartussek, in *Nonlinear Physics of Complex Systems*, edited by J. Parisi, S.C. Müller and W. Zimmermman (Springer, New York, 1999).

[8] J. García-Ojalvo, A. Hernández–Machado and J.M. Sancho, Phys. Rev. Lett. **71**, 1542 (1993).

[9] J.M.R. Parrondo, C. Van den Broeck, J. Buceta and F.J. de la Rubia, Physica **A 224**, 153 (1996).

[10] C. Van den Broeck, J.M.R. Parrondo and R. Toral, Phys. Rev. Lett. **73**, 3395 (1994); C. Van den Broeck, J.M.R. Parrondo, R. Toral and R. Kawai, Phys. Rev. **E55**, 4084 (1997).

[11] J. García-Ojalvo, J.M.R. Parrondo, J.M. Sancho and C. Van den Broeck, Phys. Rev. **E54**, 6918 (1996).

[12] S. Mangioni, R. Deza, H. Wio, R. Toral. Phys. Rev. Lett. **79**, 2389 (1997); Phys. Rev. **E61**, 223 (2000).

[13] J. García-Ojalvo, A. Lacasta, J.M. Sancho and R. Toral, Europhysics Letters **42**, 125 (1998).

[14] M. Ibañes, J. García-Ojalvo, R. Toral and J.M. Sancho, Phys. Rev. **E60**, 3597 (1999).

[15] P. Jung and G. Mayer–Kress, Phys. Rev. Lett. **74**, 2134 (1995).

[16] F. Marchesoni, L. Gammaitoni and A.R. Bulsara, Phys. Rev. Lett. **76**, 2609 (1996).

[17] R.J.Deissler, J. Stat. Phys., **54**, 1459 (1989).

[18] M. Santagiustina, P. Colet, M. San Miguel and D. Walgraef, Phys. Rev. Lett. **79**, 3633 (1997); *ibid.*, Phys. Rev. E. **58**, 3843 (1998).

[19] M. J. Berridge, P. Lipp and M. D. Bootman, Nature Rev. Cell. Biol. **1**, 11 (2000)

[20] S. Schuster, M. Marhl and T. Höfer, Eur. J. Biochem. **269**, 1333 (2002)

[21] M.E. Gracheva, R. Toral and J.D. Gunton, J. Theor. Biology **212**, 111 (2001).

[22] M. E. Gracheva and J. D. Gunton, to be published in J. Theor. Biol. (2003)

[23] K. Prank, U. Ahlvers, F. Baumgarte, H. G. Musmann, A. von zur Mhlen, C. Schöfl and G. Brabant in Methoden der medizinischen Informatik, Biometrie, Epidemiologie in der moder-nen Informationsgesellschaft, (Eds. E. Greiser, M. Wischnewsky), MMV, Medizin-Verlag, Mnchen, p. 385-388 (1998); U. Ahlvers, F. Baumgarte, H. G. Musmann, C. Schöfl, A. von zur Muhlen, G. Brabant and K. Prank, in Proceedings of the 4th International Conference on Theory and Mathematics in Biology and Medicine, Amsterdam, p. 47 (1999)

[24] M. Bär, M. Falcke, H. Levine and L. S. Tsimring, Phys. Rev. Lett. **84**, 5664 (2000).

[25] J.W. Shuai and P. Jung, Phys. Rev. Lett. **88**, 068102 (2002).

[26] H. Kramers, Physica (Utrecht)**7**,284 (1940)

[27] J. Keener and J. Sneyd,*Mathematical Physiology*, Springer (1998)

[28] A.S. Pikovsky and J. Kurths, Phys. Rev. Lett. **78**, 775 (1997).

[29] H. Gang, T. Ditzinger, C.Z. Ning and H. Haken, Phys. Rev. Lett. **71**, 807 (1993).

[30] W. Rappel and S. Strogatz, Phys. Rev. **E50**, 3249 (1994).

[31] A. Goldbeter, G. Dupont and M.J. Berridge, Proc. Natl. Acad. Sci. USA **87**, 1461 (1990).

[32] G. Dupont, A. Goldbeter and M. J. Berridge, Cell Regul. **1**, 853 (1990). Bezprozvanny, I. and B. E. Ehrlich. 1995. The inositol 1,4,5-trisphosphate ($InsP_3$) receptor. *J. Membr. Biol.* 145:205-216.

[33] Dupont, G. and A. Goldbeter. 1993. A one-pool model for Ca^{2+} oscillations involving Ca^{2+} and inositol 1,4,5-trisphosphate as co-agonists for Ca^{2+} release. Cell Calcium 22:311-322.

[34] T.R. Chay, Y.S. Lee and Y.S. Fan, J. Theor. Biology **174**, 21 (1995).

[35] U. Kummer U, L. F. Olsen, C. J. Dixon, A. K. Green, E. Bornberg-Bauer and G. Baier, Biophys. J. **79**, 1188 (2000).

[36] Th.Tordjmann, B. Berthon, M. Claret and L. Combettes, EMBO J. **16**, 5398 (1997)

[37] Th. Tordjmann,, B. Berthon, E Jacquemin, C. Clair, N. Stelly, G. Guillon, M. Claret and L. Combettes, EMBO J. **17**, 4695 (1998)

[38] G. Dupont, Th. Tordjmann, C. Clair, St. Swillens, M. Claret and L. Combettes, FASEB J. **14**, 279 (2000)

[39] T. Höfer, Th. Biophys. J. **77**, 1244 (1999).

[40] D. Gillespie, J. of Comp. Phys. **22**, 403 (1976)

[41] D. Gillespie, J. of Phys. Chem. **81**, 2340 (1997).

[42] A. M. Höfer, S. Curci, M. A. Doble, E. M. Brown, E. M. and D. I. Soybel, Nature Cell Biol. **2**, 392 (2000).

[43] R. Caroppo, A. Gerbino, L. Debellis, O. Kifor, D. I. sSoybel, E. M. Brown, A. M. Hofer and S. Curci, EMBO J. **20**, 6316 (2001)

[44] This behavior has been found earlier in a study of a finite difference model of cardiac arrhythmias [46] as well as in a model of intracellular calcium oscillations [34] in which the hormonal stimulus was modeled by a sequence of square well pulses. However, this is the first prediction of such behavior in coupled, nonexcitable cells.

[45] C. Schöfl, G. Brabant, R. D. Hesch, A. von zur Mü, P. H. Cobbold andK. S. R. Cuthbertson, Am. J. Physiol **265**, C1030 (1993).

[46] L. Glass, M.R. Guevara and A. Shrier, Annals of the N.Y. Acad. of Science **504**, 168 (1987).

[47] R. Toral, C. Mirasso and J. D. Gunton, to be published in Europhys. Lett. (2003)

[48] C. Koch, *Biophysics of Computation*, Oxford University Press, New York (1999).

[49] L. Glass, P. Hunter and A. McCulloch, eds. *Theory of Heart*, Springer–Verlag, New York (1991).

[50] T. Kanamaru, T. Horita and Y. Okabe, Phys. Rev. E, **64**, 031908 (2001).

[51] R.C. Desai and R. Zwanzig, J. Stat. Phys. **19**, 1 (1978).

[52] A. Pikovsky, A. Zaikin and M.A. de la Casa, Phys. Rev. Lett. **88**, 050601 (2002).

[53] P. Jung and J.W. Shuai, Europhys. Lett. **56**, 29 (2001).

[54] G. Schmid, I. Goychuk and P. Hänggi, Europhys. Lett. **56**, 22 (2001).

[55] C. Palenzuela, R. Toral, C. Mirasso, O. Calvo and J. Gunton, Europhys. Letters, **56**, 347 (2001).

[56] O. Calvo, C. Mirasso and R. Toral, Electronics Letters, **37**, 1062 (2001).

[57] *Chua's Circuit: A Paradigm for Chaos*, R.N. Madan, ed. World Scientific Publishing (1993).

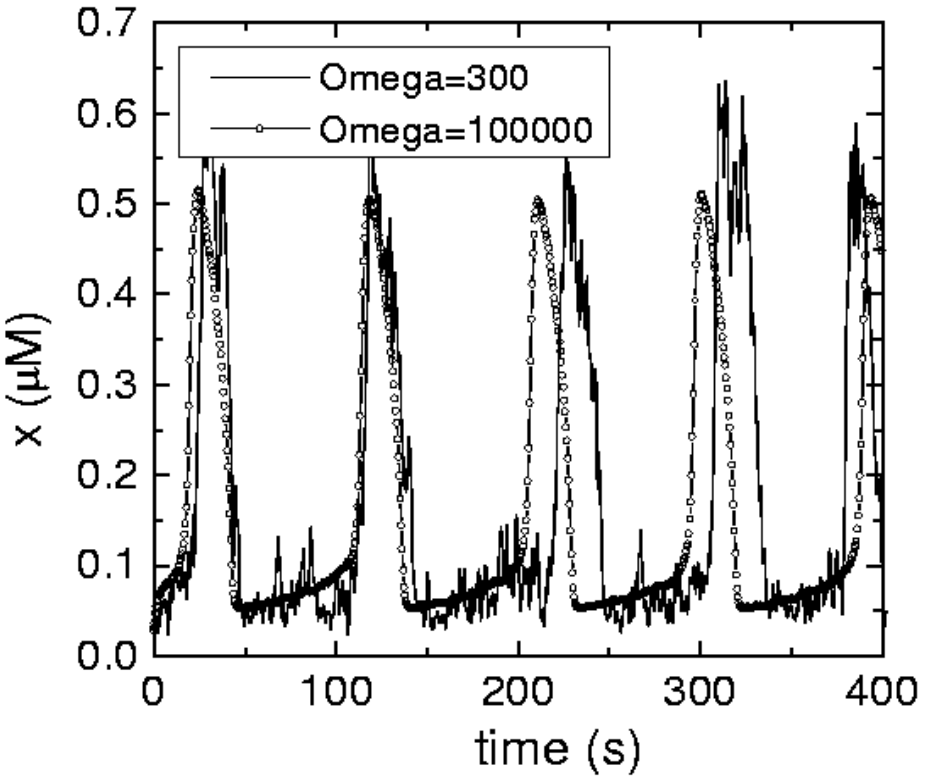

Figure 1: Calcium oscillations in the stochastic version of Höfer's model for a single cell, $N = 1$, for different values of the volume $\Omega = 300\ \mu m^3$, $10^5\ \mu m^3$. We observe that the deterministic limit is already achieved for $\Omega = 10^5$. We have taken as initial condition for the cell the resting state without agonist, $P = 0\mu$M.

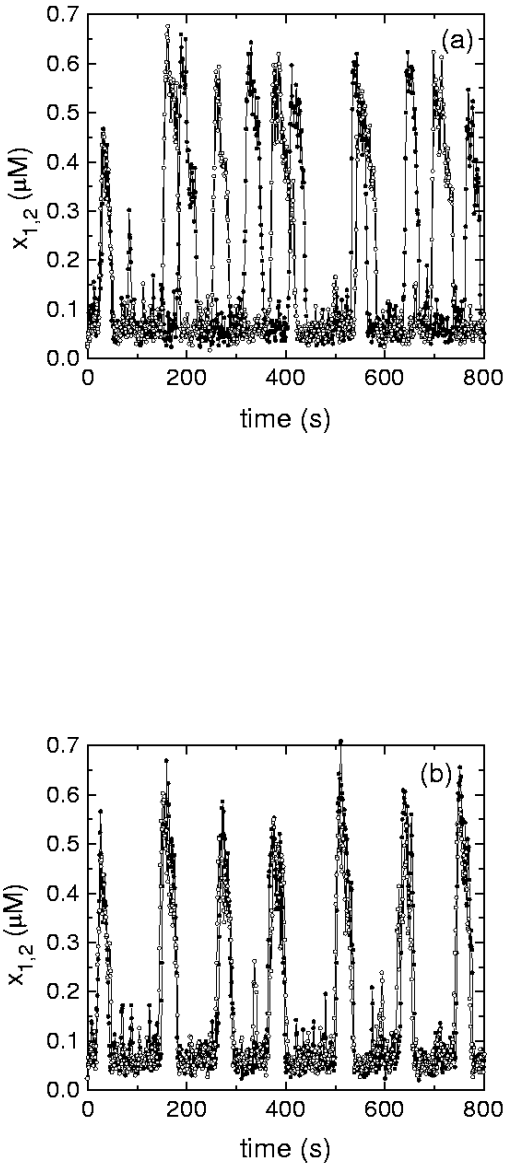

Figure 2: Calcium oscillations for a doublet of cells, $N = 2$, for different values of the permeability constant γ: (a) $\gamma = 0s^{-1}$, (b) $\gamma = 0.07s^{-1}$. Parameters: $\rho_1 = \rho_2 = 0.02$, $\beta_1 = 0.15$, $\beta_2 = 0.2$, $P_1 = P_2 = 2.0$ and the cell volume is $\Omega = 300\ \mu m^3$.

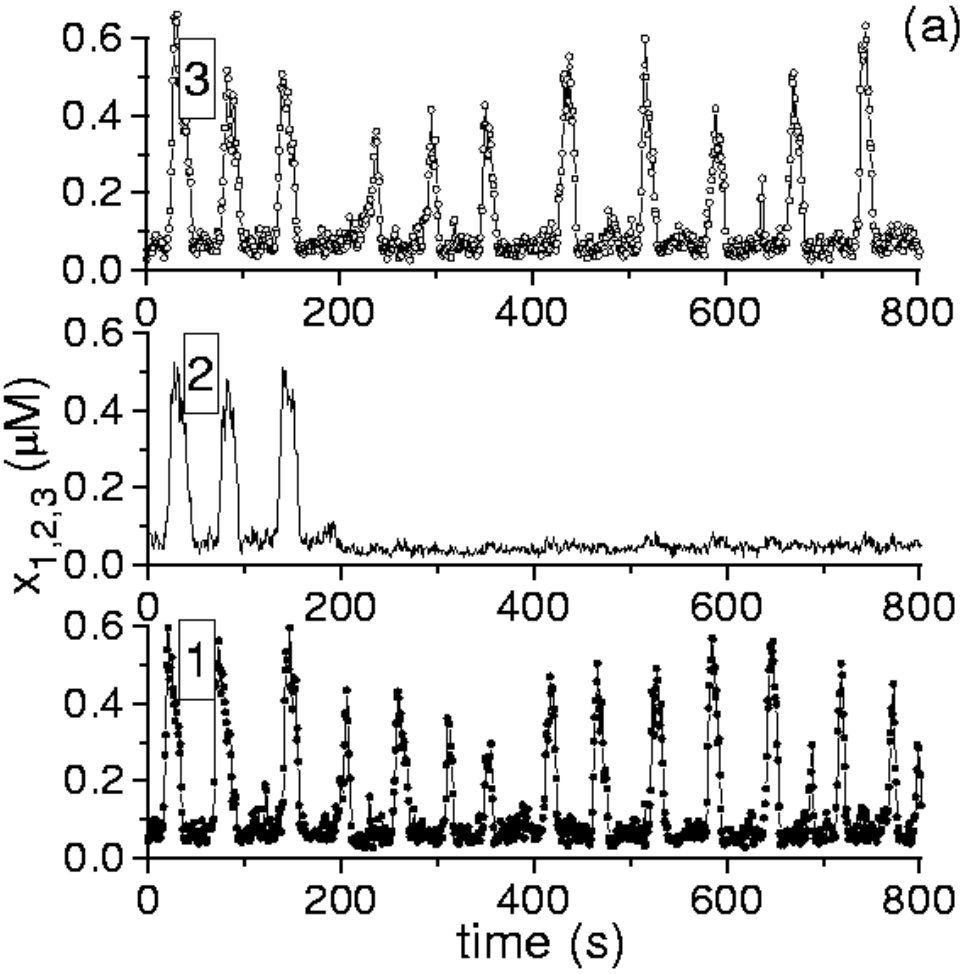

Figure 3: Simulation of heparin treatment for middle cell in the stochastic version of Höfer's model for a cell triplet, $N = 3$. The treatment starts at time=200s. We have used the following parameters: $P_2 = P_2 = P_3 = 2\mu$M, $\rho_1 = 0.025$, $\rho_2 = 0.018$, $\rho_3 = 0.02$, $\beta_1 = \frac{\beta_2}{25} = \beta_3 = 0.1$, $\gamma = 0.07 s^{-1}$. We plot the time series of the variables x_1, x_2 and x_3 in the case with $\Omega = 300\ \mu m^3$ where stochastic effects are important; treatment starts at time=200s.

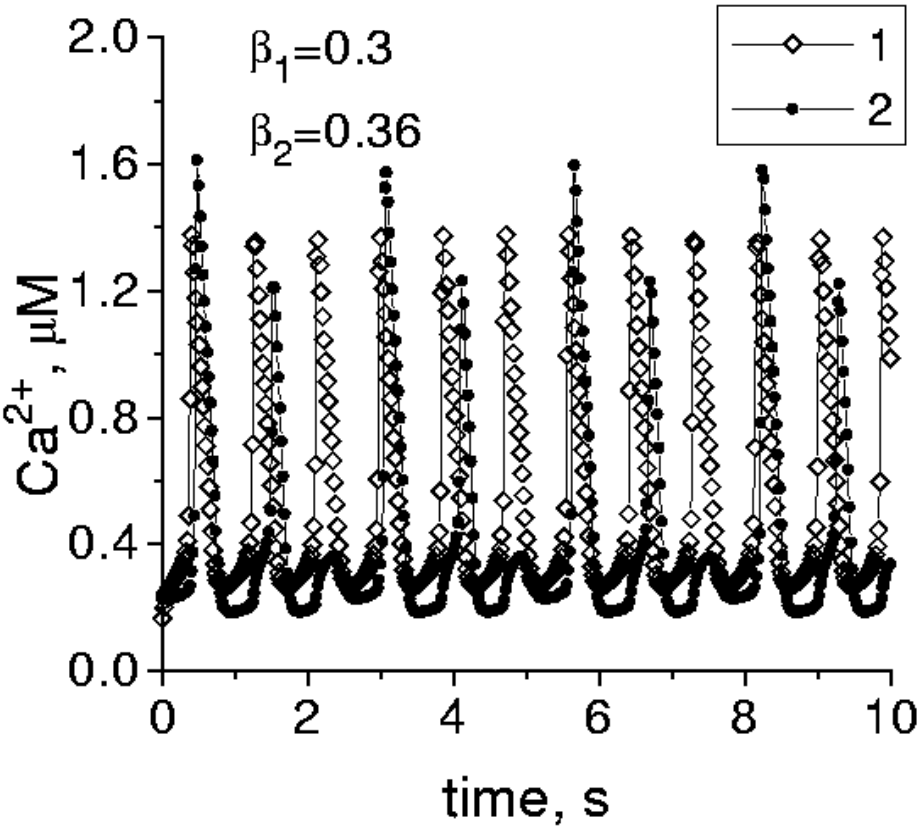

Figure 4: Calcium oscillations of two connected cells (β_1=0.3, β_2=0.36). Frequencies of cells are locked in a sequence of 3:2. Deterministic model.

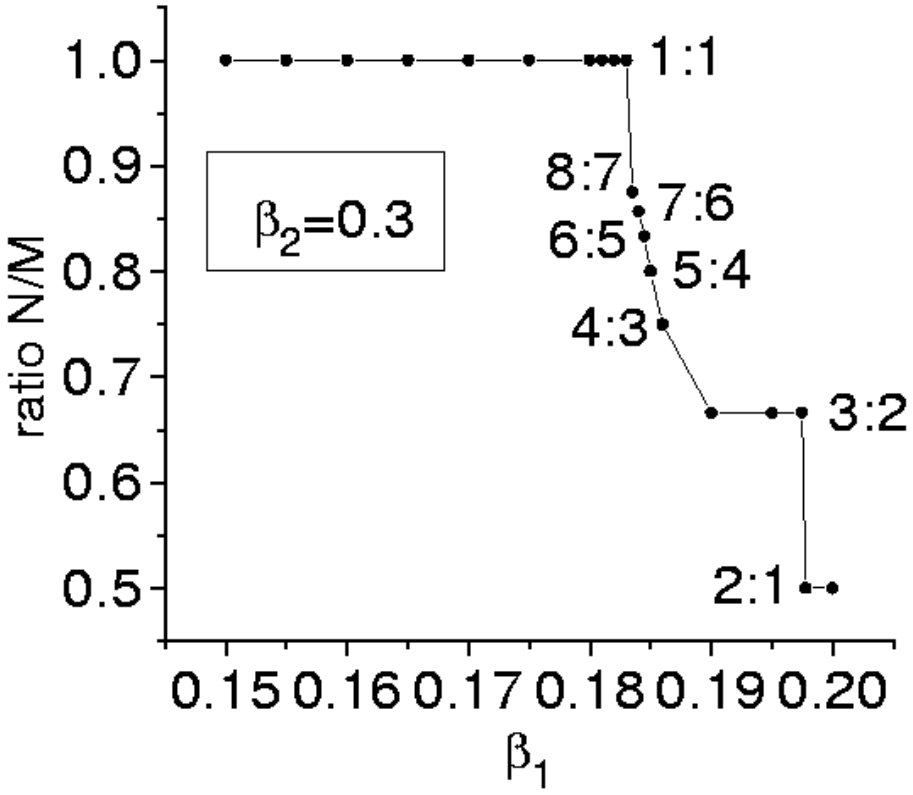

Figure 5: Devil's staircase, a ratio N/M (where N is the number of spikes of the donor cell and M is the number of spikes of the sensor cell) as a function of β_1 at fixed β_2=0.3.

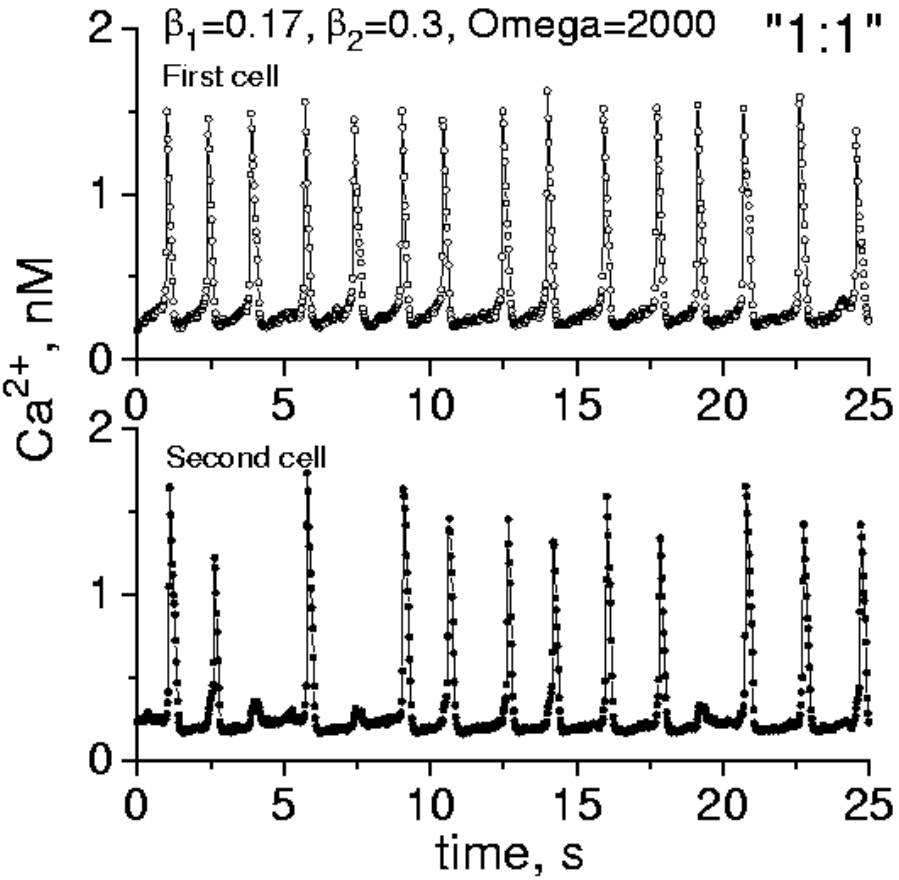

Figure 6: Calcium oscillations of two connected cells (β_1=0.17, β_2=0.3). Frequencies of cells are locked in a sequence of 1:1 with occasional fluctuations. Stochastic model with $\Omega = 2000$.

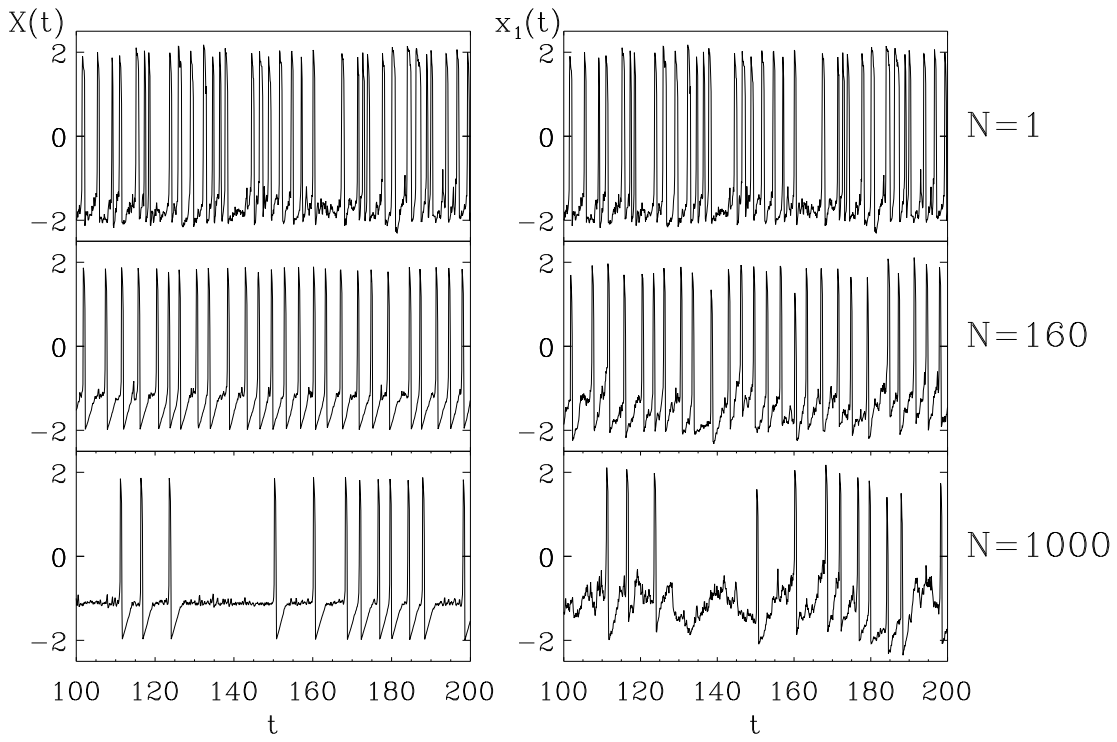

Figure 7: Time series for the averaged variable $X(t)$ (left panel), and for the individual variable $x_1(t)$ (right panel) of the set of coupled FitzHugh–Nagumo systems, as obtained from a numerical integration of Eqs.(6-7), for different values of the number of coupled elements: $N = 1$ (top), $N = 160$ (middle) and $N = 1000$ (bottom). Observe that the largest regularity is obtained for the intermediate value of N. The equations have been integrated numerically using a stochastic Runge–Kutta method (known as the Heun method [1]) with a time step $h = 10^{-4}$ and setting the following parameters: $a = 1.1$, $\epsilon = 0.01$, $K = 2$, $D = 0.7$.

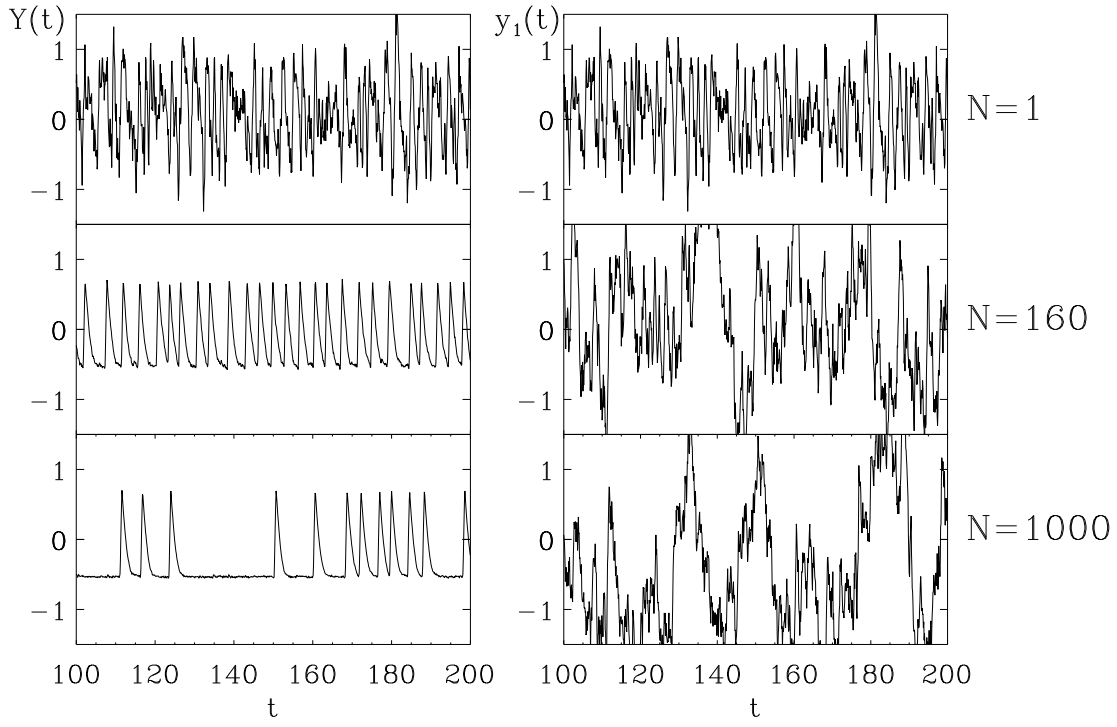

Figure 8: Time series for the averaged variable $Y(t)$ (left panel), and the individual variable $y_1(t)$ (right panel) of the set of FitzHugh–Nagumo systems, Eqs.(6-7). Similarly as in Figure 8, observe that again the largest regularity for the averaged Y variable is obtained for the intermediate value of N. In this case, however, there is no obvious increase in the regularity of the y_i individual variables.

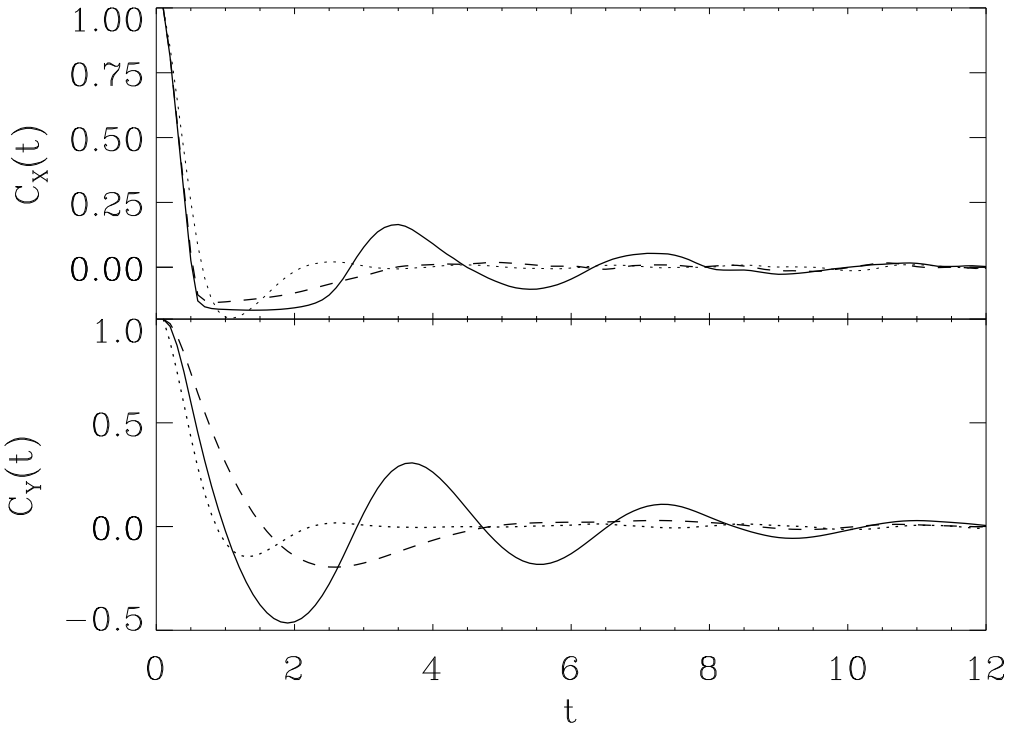

Figure 9: Correlation functions $C_X(t)$ and $C_Y(t)$ of the averaged variables $X(t)$ and $Y(t)$, respectively, for the cases of $N = 1$ (dotted line), $N = 160$ (solid line) and $N = 1000$ (dashed line). Notice that, in agreement with the qualitative results derived from figures 7 and 8, the slower decay of the correlations corresponds to the intermediate values of the system size N. Same parameters as in figure 7.

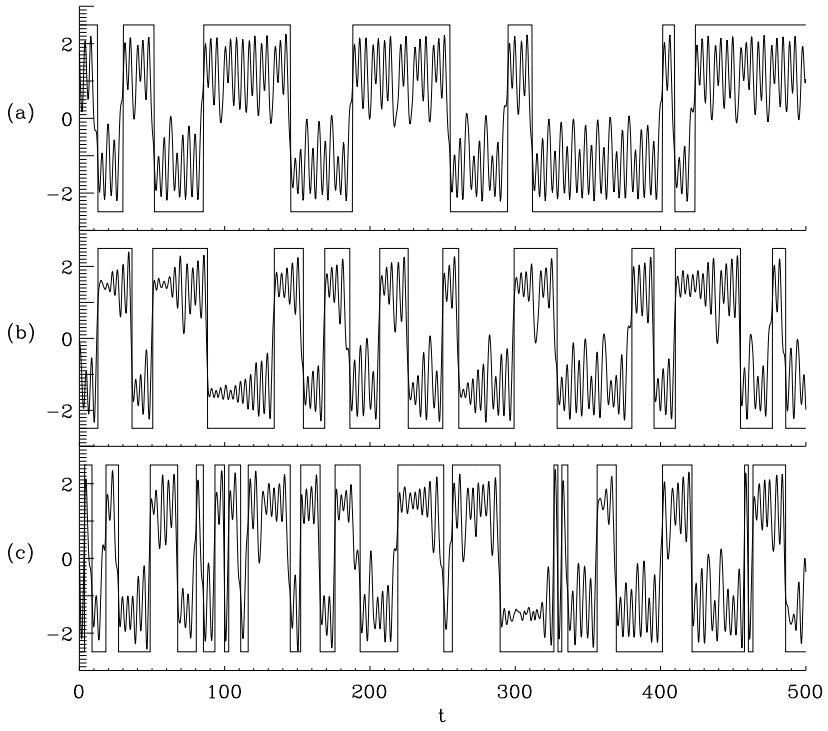

Figure 10: Time series for the x variable of the Chua system given by Eqs. (16) for three different noise levels: a) $D = 0.02$, b) $D = 0.08$, optimum noise level, and c) $D = 0.16$.

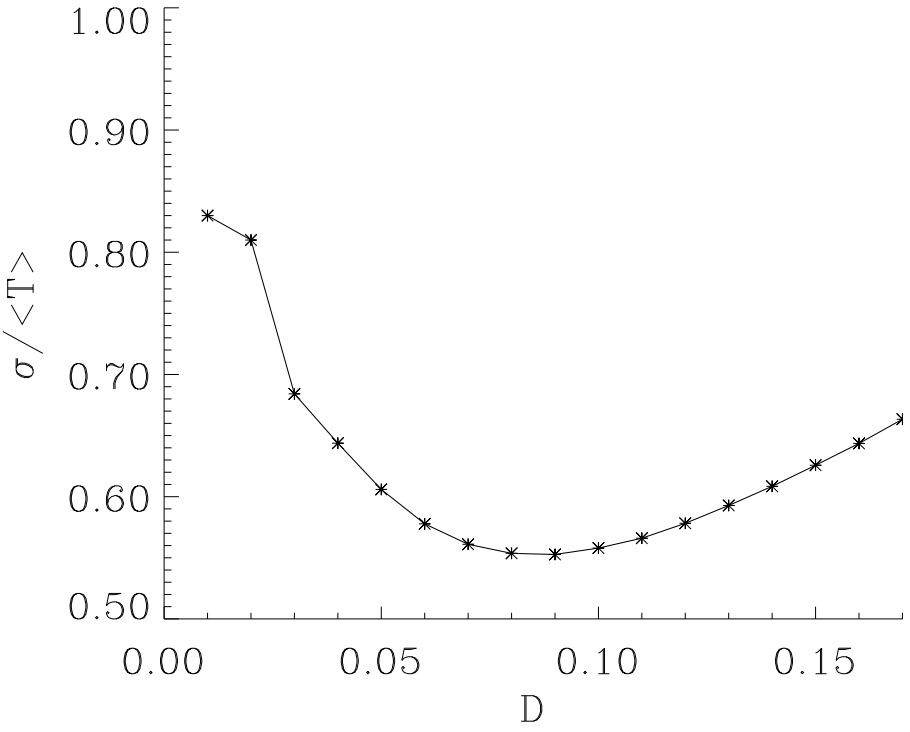

Figure 11: Standard deviation normalized by the mean time $\sigma/\langle T\rangle$ for the Chua system given by Eqs. (16) for noise levels ranging from 0.01 to 0.17.